MRI Safety Assessment of a Generic Deep Brain Stimulator

Eugenia Cabot[1], ***Tom Lloyd***[2], ***Andreas Christ***[1], ***Wolfgang Kainz***[3], ***Mark Douglas***[1], ***Gregg Stenzel***[2], ***Steve Wedan***[2], and ***Niels Kuster***[1,4]

[1] IT'IS Foundation, Zeughausstr. 43 8004 Zurich, Switzerland, cabot@itis.ethz.ch
[2] Imricor Medical Systems, 400 Gateway Blvd, Burnsville, MN 55337, USA
[3] FDA, 10903 New Hampshire Avenue, Silver Spring, Maryland 20993-0002, USA
[4] Swiss Federal Institute of Technology (ETHZ), ETH Zentrum ETZ, 8092 Zurich, Switzerland

Abstract

The radio frequency (RF) electromagnetic field of magnetic resonance (MR) scanners can result in significant tissue heating due to the RF coupling with the conducting parts of medical implants. The objective of this paper is to assess the safety of a generic deep brain stimulator (DBS) during MRI scans based on a combined numerical and experimental procedure described in [1]. The evaluation is performed for 1.5 T MR scanners using a generic model of a deep brain stimulator with a helical lead. The results show that the approach is technically feasible and provides sound and conservative information on the potential heating of implants.

1 Introduction

The importance of MR diagnostics is continuously growing because of the improved soft tissue contrast and the absence of ionizing radiation compared to conventional computer tomography, and because of novel high resolution techniques. However, patients with electrically conductive implants are generally excluded from MR diagnostics due to the interference with the RF-fields, which can cause imaging artifacts, spurious tissue heating and EMC/EMI issues. A summary of the most relevant aspects of the MR safety of implants can be found, e.g., in [2, 3]. Active implants with electrically long and insulated leads, such as pacemakers and DBS, are of particular concern because they pick up electromagnetic (EM) energy along their entire length, which gives rise to a highly localized increase in the electric field strength and the specific absorption rate (SAR) in the patient's tissue surrounding the electrodes of the device. These issues have been recognized by a joint working group of the ISO TC 150/SC6 and the IEC 62B MT40 and a Technical Specification (JWG ISO/IEC TS) for the demonstration of the MR safety of active implanted medical devices (AIMDs) for patients undergoing MR diagnostics at 1.5 T is being developed [1]. The objective of this study is to evaluate the applicability, advantages and shortcomings of the approach proposed in the JWG ISO/IEC TS technical note [1]. The procedures are tested for a generic model of a DBS which reproduces the typical RF characteristics of such a device.

2 Methods

Generic Deep Brain Stimulator: The generic DBS developed here consists of a stainless steel stimulator can of size 25 mm×3 mm×40 mm and a dielectric header (ϵ_r=3) of size 25 mm×3 mm×10 mm. The stimulator can be equipped with an insulated helical copper lead with a pitch of 0.33 mm, a radius of 0.5 mm, and a wire diameter of 0.13 mm. The lead passes through the header, and is directly connected to the can supposing perfect grounding of the RF currents on the lead (Figure 1). The topology of the lead is constant along its entire length. The distal end of the lead is terminated with a bare cylindrical copper tip with a radius of 0.5 mm and a length of 10 mm. For experimental validation, the implant has been built with 4 different lead lengths: 50 mm, 100 mm, 150 mm and 200 mm.

Simulation Method: The simulations were performed with SEMCAD X V14 (Schmid & Partner Engineering AG, Switzerland), based on the finite-difference time-domain (FDTD) method [4].

978-1-4244-6051-9/11/$26.00

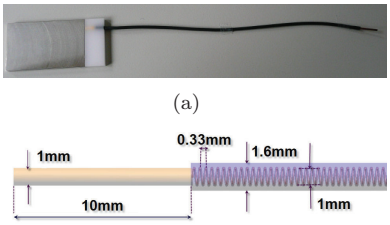

(a)

(b)

Figure 1: (a) Generic DBS model consisting of a stainless steel can, a dielectric header and a generic insulated helicoidal lead. (b) Dimensions of the helical lead and the tip.

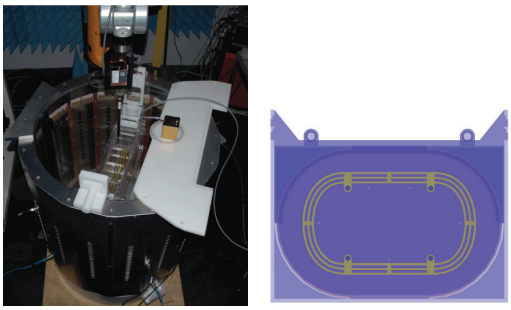

(a) MITS 1.5. (b) ELIT 1.5.

Figure 2: MITS 1.5 system and CAD of the ELIT 1.5 phantom.

Measurement and Exposure Systems: The implant is exposed to RF using the Medical Implant Test System MITS 1.5 (Zurich MedTech (Switzerland)), which reproduces the RF field of a large volume birdcage resonator of commercial MR scanners. The birdcage resonator is tuned to 64 MHz and can be operated in linear and in quadrature mode. For the exposure of the generic implant to a well-defined incident E-field, a special phantom has been developed. The induced SAR and temperature distribution is evaluated using the Dosimetric Assessment System DASY 52 NEO (Schmid & Partner Engineering AG, Switzerland) equipped with H-field (H3D7V), E-field (ER3DV5), SAR (EX3DV6) and temperature (T1DV2) probes. The MITS 1.5 measurement system and the phantom are shown in Figure 2.

3 Results

Validation of Measurement and Exposure Systems: In order to validate the experimental setup, E-field, H-field and SAR are evaluated along the bore axis of the MITS 1.5 birdcage resonator, in the elliptical phantom ELIT 1.5 filled with high conductivity medium ($\epsilon_r = 78$ and $\sigma = 0.47\,\mathrm{S/m}$). Figure 3 shows the measured and simulated results on the bore axis. In general, the agreement between experimental and numerical results is good.

To evaluate the performance of the measurement system for the assessment of the highly confined fields at the implant tips, [1] defines a straight insulated wire as a generic implant for a benchmark test and provides reference results. The wire has a length of 200 mm and a diameter of 1.5 mm. It is insulated by a 0.5 mm thick dielectric. At the tips, the insulation is removed over a length of 10 mm. For the validation of the measurement system, the wire is positioned on the mounting track, and the SAR distribution at its tip is measured and compared to the reference results provided in [1]. Figure 4(a) shows the comparison of the measured and simulated SAR in the radial direction at a distance of 2 mm and 5 mm from the tip normalized to the E-field in the background. The measured results are within ±0.9 dB of the reference results, which is satisfactory for the application of the system. For the validation of the numerical model of the generic DBS, the measured and the simulated SAR at the lead tip are compared for different lengths of the helical lead in 50 mm increments, i.e., 50 mm, 100 mm, 150 mm and 200 mm. Figure 4(b) shows measured and simulated SAR for the lead of length 100 mm in the radial direction at distances of 2 mm and 5 mm from the tip normalized to the incident tangential E-field at the location of the implant. The maximum difference of all experimental evaluations from the numerical results is 1.7 dB. This is less than the combined absolute uncertainties of 2.8 dB ($k = 2$), thus the numerical model of the implant can be considered valid for the purpose of this study.

Energy Deposition *In Vivo* for the Helical and the Straight Lead: The validated DBS is positioned in the head model of Duke ([5],[6]) following a realistic routing path. The stimulator can is placed in a typical

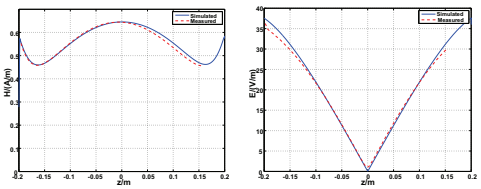

(a) H_{rms} (b) E_{rms}

Figure 3: Measured vs. simulated H_{rms} and E_{rms} along z-axis in the ELIT 1.5, for x=0, y=0 at 1.5 T.

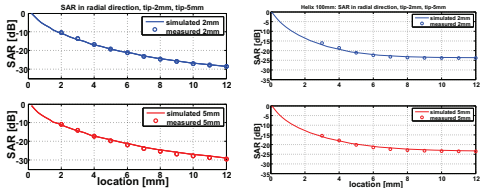

(a) Straight wire (b) Helix

Figure 4: Measured vs. simulated SAR distribution extracted in the radial direction, at 2 mm and 5 mm from the tip end of the benchmark wire (4(a)) and the 100 mm long implant with helical lead (4(b)).

position above the skull behind the right ear of the model. The lead is tunneled subcutaneously toward the top of the head where it traverses the skull and penetrates the cortex. The tip of the lead ends in the thalamic region. Figure 5 shows the position of the implant and the trajectory of the lead in the anatomical model in detail. The dielectric parameters of the tissues are chosen according to [7]. The implanted head is positioned in the center of the birdcage coil. The exposure of the implant in the head is simulated in a two step process using the Huygens box approach [8]. Figure 6(a) shows the SAR distribution at the lead tip. The $psSAR_{10\,mg}$ at the tip of the implant is 4.95 W/kg/μT^2, and the SAR averaged over the total mass of the head is 0.068 W/kg/μT^2. This permits the exposure of the patient to a B_1-field of 6.9 μT to reach the limit of 3.2 W/kg (Normal Mode and First Level Controlled Mode). Normalizing the $psSAR_{10\,mg}$ of 4.95 W/kg/μT^2 to this incident magnetic field yields a $psSAR_{10\,mg}$ of 0.23 kW/kg. The numerical uncertainty estimated to be 1.1 dB. The overall expanded uncertainty including the experimental and numerical evaluation is 4.2 dB for a coverage factor k of 2. It should be noted that this does not cover the variability of the exposure due to changes in patient anatomy, exposure position and lead trajectory.

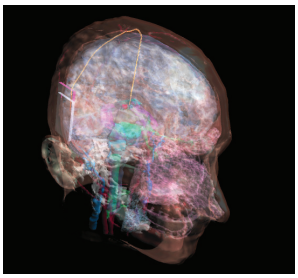

Figure 5: Positioning of the DBS in the human head model (insulation of the lead not shown).

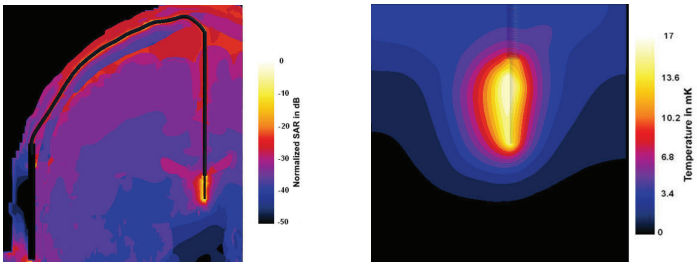

(a) SAR distribution (b) Temperature distribution

Figure 6: SAR and temperature distributions at the tip of the DBS when implanted in the Duke's head, positioned in the center of 1.5T birdcage coil.

Determination of the *In Vivo* Transfer Function SAR to Temperature: In order to correlate the localized power (SAR) deposition to a potential hazard, i.e., local temperature rise, the transfer function SAR to ΔT must be determined. In the vicinity of the tip, the most prominent tissues and brain regions are the thalamus, grey and white matter, midbrain and cerebrospinal fluid (CSF). In order to determine the sensitivity of the maximum temperature increase to the uncertainties of the tissue parameters and of the cooling due to the temperature conduction of the lead, two scenarios were evaluated using the steady-state thermal solver of SEMCAD X and the head model Duke: considering the conductivity of the metal and neglecting the conductivity of the metal. A conservative temperature rise of 17 mK/(μT)^2 is obtained when the conductivity of the metallic parts of the lead is neglected. The temperature rise is 12% lower when considering the heat dissipation produced by the metal conductivity. The temperature increase at the

Normal and First Level Controlled Modes limit is 0.8 K. Therefore this yields a conservative transfer function coefficient of 3.6mK/W/kg. Figure 6(b) shows the temperature distribution at the lead tip.

4 Conclusions

The RF safety in MRI environment of a generic DBS has been assessed according to the procedures presented in [1]. First, the numerical model of the DBS has been validated vs. measurements in a homogeneous phantom. Then, the device has been implanted in a human model and EM and thermal simulations have been run. The results show that the approach proposed in [1] is technically feasible and provide sound and conservative information about the potential heating produced by the implant under MRI conditions.

5 Acknowledgements

This study was generously supported by the Medical Devices Research Forum (MDRF), Burnsville, MN.

References

[1] ISO/TC150/SC6/JWG2 and IEC SC62B/JWG1, *Requirements for the safety and compatibility of magnetic resonance imaging for patients with an active implantable medical device*. International Organization for Standardization, 2010. Draft International Technical Specification for ISO/TS 10974.

[2] E. Martin, J. Coman, F. Shellock, C. Pulling, R. Fair, and K. Jenkins, "Magnetic resonance imaging and cardiac pacemaker safety at 1.5-Tesla," *Journal of the American College of Cardiology*, vol. 43, no. 7, p. 1315, 2004.

[3] J. Nyenhuis, S. Park, R. Kamondetdacha, A. Amjad, F. Shellock, and A. Rezai, "MRI and implanted medical devices: basic interactions with an emphasis on heating," *IEEE Transactions on device and materials reliability*, vol. 5, no. 3, p. 467, 2005.

[4] A. Taflove and S. C. Hagness, *Computational Electromagnetics: The Finite-Difference Time-Domain Method*. Boston, USA, London, United Kingdom: Artech House, Inc., second ed., 2000.

[5] A. Christ, W. Kainz, E. G. Hahn, K. Honegger, M. Zefferer, E. Neufeld, W. Rascher, R. Janka, W. Bautz, J. Chen, B. Kiefer, P. Schmitt, H.-P. Hollenbach, J. Shen, M. Oberle, D. Szczerba, A. Kam, J. W. Guag, and N. Kuster, "The Virtual Family – Development of surface based anatomical models of two adults and two children for dosimetric simulations," *Phys. Med. Biol.*, vol. 55, pp. N23–N38, 2010.

[6] Virtual Population, http://www.itis.ethz.ch/services/human-and-animal-models/human-models/

[7] S. Gabriel, R. W. Lau, and C. Gabriel, "The dielectric properties of biological tissues: III. Parametric models for the dielectric spectrum of tissues," *Phys. Med. Biol.*, vol. 41, pp. 2271–2293, Nov. 1996.

[8] S. Benkler, N. Chavannes, and N. Kuster, "New powerful FDTD source based on huygens surface: Highly complex EM simulations performed on an ordinary PC." Poster at the 31th Annual Meeting of the Bioelectromagnetics Society (BEMS 2009), Davos, Switzerland, June 14–19, 2009.